CGH-LUPI interferometer for aspheric figure metrology

Steven M. Arnold, Andrew P. Stuart, Lubomir Koudelka

Steven M. Arnold, Andrew P. Stuart, Lubomir Koudelka, "CGH-LUPI interferometer for aspheric figure metrology," Proc. SPIE 3134, Optical Manufacturing and Testing II, (1 November 1997); doi: 10.1117/12.295152

SPIE.

Event: Optical Science, Engineering and Instrumentation '97, 1997, San Diego, CA, United States

CGH-LUPI Interferometer for Aspheric Figure Metrology

Steven M. Arnold[a], Andrew P. Stuart[a], and Lubomir Koudelka[b]

[a]Diffraction International Ltd., 11345 Highway 7, #421, Minneapolis, MN 55303[1]
[b]Promet International Inc., 4611 Chatsworth Avenue, Shoreview, MN 55126[2]

ABSTRACT

We have designed and built a phase-measuring LUPI interferometer to use pre-aligned custom CGH nulls for high accuracy figure metrology of deep aspherics. The CGH nulls operate in double pass, first producing an aspheric test wavefront and then re-collimating the return wavefront. This eliminates any need to locate the CGH at an image of the test pupil. The CGH is common to both test and reference paths, allowing the use of photomask quality substrates.

To enable the CGH-LUPI to test a wider variety of aspheres, we have designed and built a set of 100 mm aperture accessory optics for use in combination with CGH nulls. These accessory optics consist of five singlets, each approximately F/3, which may be kinematically stacked in numerous combinations and permutations to produce test wavefronts ranging from nearly collimated to F/0.75. A CGH null compensates for asphericity of the test optic and design aberrations of the accessory optics.

The interferometer and accessory optic designs permit independent verification of all aspects of system accuracy and calibration without the need for disassembly. Designing a custom CGH null involves raytracing the accessory optics but not the interferometer mainframe optics. Depending on the phase measuring algorithm selected, known system aberrations due to manufacturing tolerances may be software compensated in real time.

Keywords: aspheric metrology, interferometry, optical testing, CGH

1. TECHNICAL OBJECTIVES

We have set several technical goals for ourselves in designing and building this instrument:

- Test deep general aspherics, up to 1000 waves per radius (slope)
- Use prealigned, photomask quality CGH nulls
- Verify calibration without disassembly
- Intelligent "real time" phase measuring
- "Walkup" aspheric test capability.

We favor photomask quality CGH nulls because they can be made quickly and accurately by e-beam lithography and are fairly inexpensive. Calibration without disassembly is important if the instrument is to gain acceptance as an aspheric metrology tool; previous CGH interferometers have required blind faith on the part of the user. Intelligent real-time phase measuring requires the computer to do more than just drive a DAC board and process the video data. The computer should know what is being tested, control the interferometer zoom, focus and intensity, and perform or at least assist with the alignment. Finally, walkup aspheric interferometer[1] refers to an ability to test an aspheric surface without the need to first prepare a custom null or reference.

2. INTERFEROMETER MAINFRAME

2.1 Overview

Figure 1 shows a nearly complete prototype of the interferometer mainframe with cosmetic and dust covers removed. It is built on a 400 mm x 450 mm optical breadboard.

---

1 Further Diffraction International information: Email: steve@diffraction.com or andrew@diffraction.com, Telephone: 612-945-9912, Fax: 612-945-9935

2 Further Promet International information -- Email: promet@winternet.com, Telephone: 612-481-9661, Fax: 612-481-9565

SPIE Vol. 3134 • 0277-786X/97/$10.00

The optical schematic, depicted in Figure 2, is a modified Twyman-Green or LUPI type configuration. The HeNe laser source, after passing through a small beamsplitter cube and being expanded to Ø48 mm and collimated, is incident on the CGH null. The CGH has a 62.5 lpmm linear carrier and functions as a grating beamsplitter, diffracting and reshaping the test beam while passing the collimated reference beam. A reflective second beamsplitter exists only to redirect the test beam—that it again splits both test and reference beams is an unwanted side effect. The returning test beam is diffracted a second time by the CGH null, combining with the returning reference beam to form a nominally null interferogram. The small beamsplitter cube routes the returning test and reference beams to the viewing arm. In the following sections, we describe in more detail key subassemblies of the CGH-LUPI interferometer.

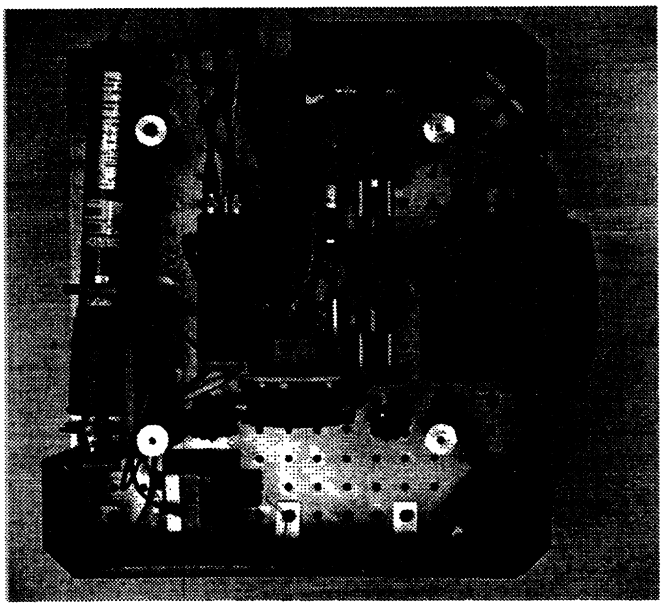

Figure 1. CGH-LUPI mainframe with cover removed.

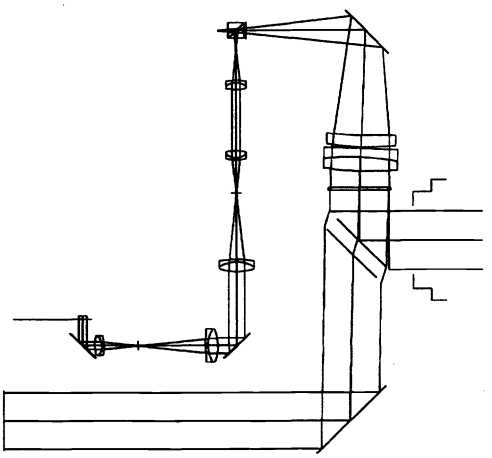

Figure 2. Optical schematic.

This interferometer design offers key advantages over previous configurations which have located a CGH either in the viewing arm[2,3] or in the test arm[4]. Specifically, the CGH null is both double pass and common path. Double pass means the test beam can be a true null wavefront which will retrace itself. This eliminates the need for imaging the test pupil onto the CGH to prevent wavefront shearing. Common path is important because it reduces the need for CGH substrates of highest optical quality—photomask quality will suffice.

The principle disadvantage of this interferometer design is that the many extraneous diffracted, reflected and transmitted beams reduce the intensity available at the camera and cam result in visible ghost fringes if not carefully managed.

2.2 CGH Beamsplitter Assembly

Figure 3 is indicative of how the CGH nulls are prealigned in individual frames which attach kinematically to a mounting surface by means of hardened steel balls, carbide rods, and magnets. An individual CGH can easily be removed and replaced with virtually no change in alignment, while multiple CGHs can be similarly aligned to within a few microns. Additionally, the alignment of CGHs in their frames is readily verified using only a dial gauge to check coplanarity and a microscope with reticle to check consistency of alignment in the plane of the CGH (by means of integral fiducial marks).

Figure 4 shows most of the CGH beamsplitter assembly. The reflective beamsplitter itself is omitted for better visibility. The location of the CGH frame is determined by the fixed kinematic mount. A hinged loading mechanism allows CGHs to be ejected from and inserted into an opening in the top of the instrument. An accessory bayonet provides for kinematic mounting of accessory optics with the ability to clock them in increments of 120 degrees. The source collimation lens is mounted to one of the bayonet support brackets and the reference beam passes through the opposite support bracket. Also omitted from the figure is a sheet metal cover which prevents dust, which might enter the bayonet opening, from migrating beyond the first beamsplitter surface and the final collimation lens surface.

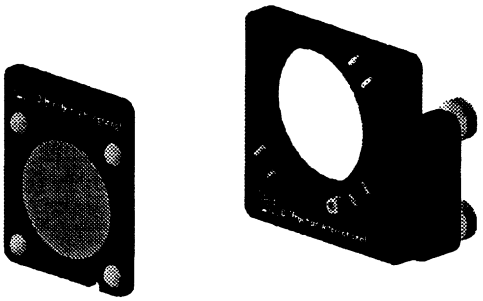

Figure 3. Prealigned CGH and kinematic mount.

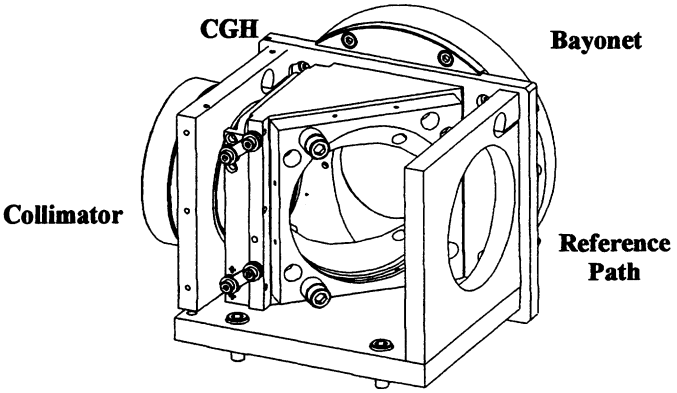

Figure 4. CGH beamsplitter assembly.

The critical alignments here are 1) collimation and aiming of the source beam with respect to the CGH and 2) alignment of the accessory bayonet with respect to the diffracted test beam. Source collimation is readily verified using a shear plate or similar. Aiming of the source beam is verified by inserting a CGH of twice the nominal carrier frequency so that it will retroreflect a portion of the source beam, making null interference fringes with a portion of the test beam retroreflected by a corner cube.

Optical alignment of the accessory bayonet to the CGH requires six degrees of freedom. Three are provided by the three 80-TPI screws on the beamsplitter frame and another three by decentering and clocking the bayonet face plate where it bolts to the assembly. Alignment verification is by means a reflective alignment CGH which attaches to the bayonet and a corresponding CGH null. The CGH null aperture is divided into six pie shaped segments, three of which produce a diverging spherical wavefront and 3 of which produce a converging spherical wavefront. The reflective alignment CGH has six corresponding zone plate aperture segments which act as simultaneous return spheres for the diverging and converging spherical wavefronts. Additionally, the alignment CGH includes a linear grating aperture which retroreflects that portion of the reference beam, undiffracted by the CGH, which is reflected to the test arm by the beamsplitter.This gives clock verification.

That the reflective alignment CGH is truly centered on the accessory bayonet can be verified by clocking the fixture in increments of 120 degrees and noting any tilt or defocus fringes in the various interferogram segments.

2.3 Reference Arm and Ghost Management

Because the CGH null works in double pass and has several diffraction orders, ghosts are a very real issue. This is particularly a problem when the CGH has little optical power so it is almost a linear grating. The reference wavefront is supposed to pass undiffracted through the CGH twice. However, the +1st order diffracted wavefront transmitted by the beamsplitter into the reference path is separated in angle from the reference wavefront, but upon its return a portion is diffracted into the –1st order which is then exactly parallel to the reference wavefront. Similarly for the outbound –1st order wavefront which diffracts into +1st order on its return. And the same is true of the ±3rd order wavefronts and any other combinations which sum to zero. A similar problem exists for test path wavefronts whose diffraction orders sum to two. The even non-zero orders are nearly absent for a Ronchi ruled CGH, but the –1st and +3rd orders will add to two, as will the +3rd and –1st orders. In the case of testing a flat, we will have five or more parallel reference path wavefronts and three or more parallel test path wavefronts! Additionally, we can expect a slight amount of 2nd order reflection off a chrome CGH, exactly parallel to the test and reference wavefronts.

Fortunately, the angular separation of the unwanted diffraction orders can enable them to walk off the CGH aperture before the second diffraction can occur. This requires that the test and reference paths each be long enough (>606 mm) for the walk off to be total (>48 mm). Figure 5 shows a raytrace simulation of the ghost problem for the testing of a flat. The bright ghosts at the right and left edges of the aperture are from the reference path of length 480 mm. The dimmer ghosts which cover most of the aperture are from the much shorter path, length 100 mm; they are not a critical problem since we can always lengthen the test path to increase their walk off.

In the case of aspheric CGH nulls, the diffraction ghosts will generally walk across the aperture to a region where the local grating period is different enough that they are not diffracted parallel to the desired test and reference wavefronts. We find that about ±100 wave of focal power in the CGH is enough to extinguish reference path ghosts. Except for the case of testing a flat or

near flat with no accessory optic, we are always able to translate the test optic along the optic axis enough to introduce this much focal power into the CGH. Therefore, diffraction ghosts will usually not present problems if we give them adequate consideration when defining a null test configuration.

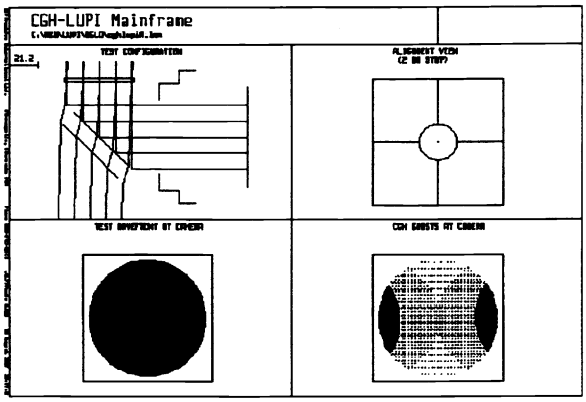

Figure 5. Diffraction ghost analysis.

It is because of diffraction ghosts that we have designed a long reference path. To give additional flexibility in suppressing reference path ghosts, we plan to mount the reference mirror on a slide so that the reference path length can be varied. This may also prove useful in balancing test and reference path lengths to within a multiple of the laser cavity length, allowing us to use a lower coherence length laser and thereby suppress any ghosts of the more conventional (reflected) sort. Phase shifting is accomplished by means of a piezo-driven flex-hinge stage under the reference path fold mirror. This stage provides linear translation free of tilt/tip without the need to balance three piezo transducers.

A final comment on the reference path. We have designed a wedged first and second surface dual reference mirror which is mounted on a pico-motor driven tilt-tip stage. This will allow us to switch between high and low reflectivity reference mirrors for both testing mirrored and uncoated aspherics. The reference mirror pico-motors will also play a role in achieving a "walk-up" aspheric testing capability—but that will be the subject of another paper.

2.4 Input Beamsplitter Assembly

Figure 6 shows the Input Beamsplitter Assembly. The linearly polarized laser source is introduced by means of a single-mode optical fiber. The small polarizing beamsplitter cube is followed by a quarter wave retardation plate. Rotation of the waveplate serves as an intensity control, causing the fraction of returning light reflected into the viewing arm to vary from nearly zero to nearly 100 percent. A variable field stop at the focus of the collimation lens serves to block unwanted diffraction orders. The viewing lens recollimates the test and reference beams at a diameter of 6.6 mm.

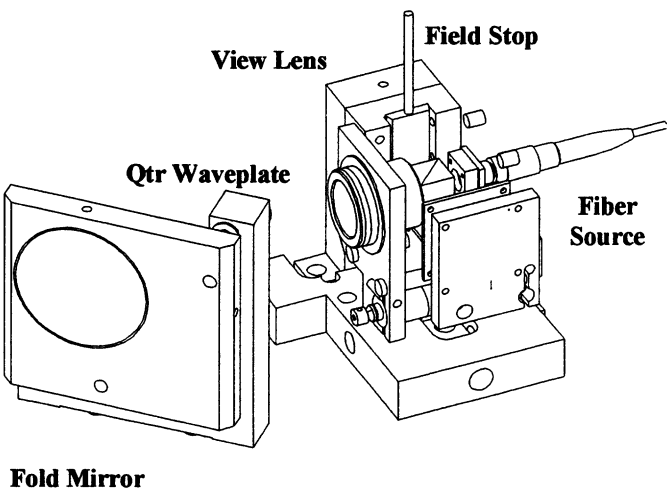

Figure 6. Input beamsplitter assembly.

An alignment camera (not shown) looks into the fourth port of the small beamsplitter through a Steinheil triple achromat to observe the fiber source and the focused images of the test and reference beams on the field stop and/or fiber bulkhead face. The fiber source provides a fixed reference for aligning both test and reference beams, a function more often provided by a corner cube.

The fold mirror mount uses three 80-TPI screws to adjust collimation and aiming of the source beam. Verification of the source collimation and aiming was discussed earlier.

2.5 Viewing Arm Assembly

Figure 7 shows the viewing arm assembly. First is a focus relay consisting of a 2X afocal telescope with 150 mm axial travel which delivers the test pupil image, located somewhere near the viewing lens, to a fixed location just prior to the following fold mirror. This design provides an exceptional ±1750 mm focus range at the Ø48 mm test beam—more if the test beam is further expanded.

Next is a zoom turret consisting of three afocal telescopes of magnifications 2X, 1.5X, and 1.15X. All three telescopes have the same object-to-image distance so that the turret provides six discrete zoom magnifications with a total range of 4:1. A pinwheel tipped with steel balls provides some adjustability of the detent angle so that image remains centered throughout the zoom range. Conveniently, the 2X zoom telescope optics are identical to the 2X focus relay telescope optics. A big advantage of discrete zoom magnifications is that the computer can know the interferogram scale factor very precisely.

After the zoom relay and a second fold mirror is a symmetrically located second pupil image at which we have located either a diffuser and afocal camera relay or else we image directly onto the camera CCD face. We have built versions using two different cameras. The first is an inexpensive 1/2-inch format, 512x512 pixel CCIR video camera. The second is a 1024x1024 pixel by 8-bit RS-422 digital camera with an option for binning to 512x512 pixels at approximately 4 times the frame rate.

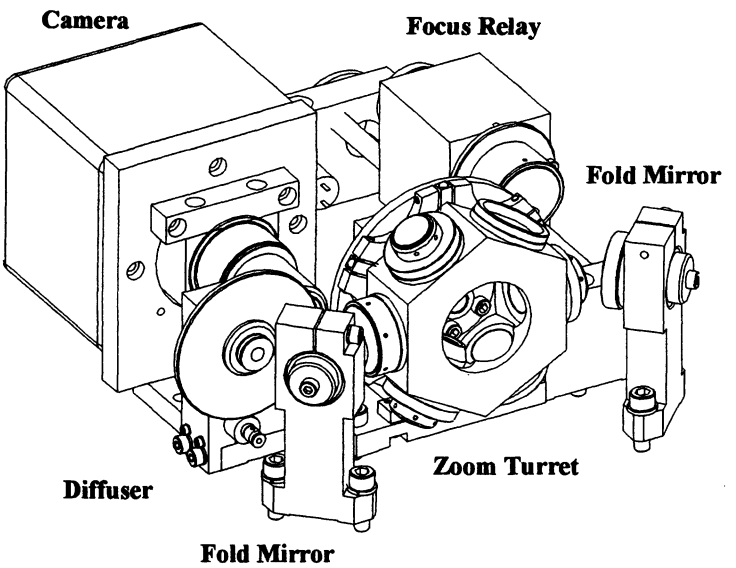

Figure 7. Viewing arm assembly.

3. ACCESSORY OPTICS

Figures 8 and 9 depict the 100 mm aperture accessory optics for the CGH-LUPI interferometer. Basically, we have a negative biconcave lens which expands the test beam, followed by one to four additional singlets which can be stacked to provide 100 mm collimated, F/3, F/1.5 or F/0.75 test beams. At this writing, we have completed only the bayonet, the 100 mm collimator and the F/3 converger accessories.

The most innovative feature about these accessory optics is that they can be stacked kinematically in nearly any combination or sequence and each element can be clocked in increments of 120 degrees. The only exception is that the barrel and flange containing the negative lens can only mount directly to the bayonet. When stacked in their 'natural' order, these elements produce fairly well corrected spherical test beams—the remaining correction (plus enough focal power to eliminate reference

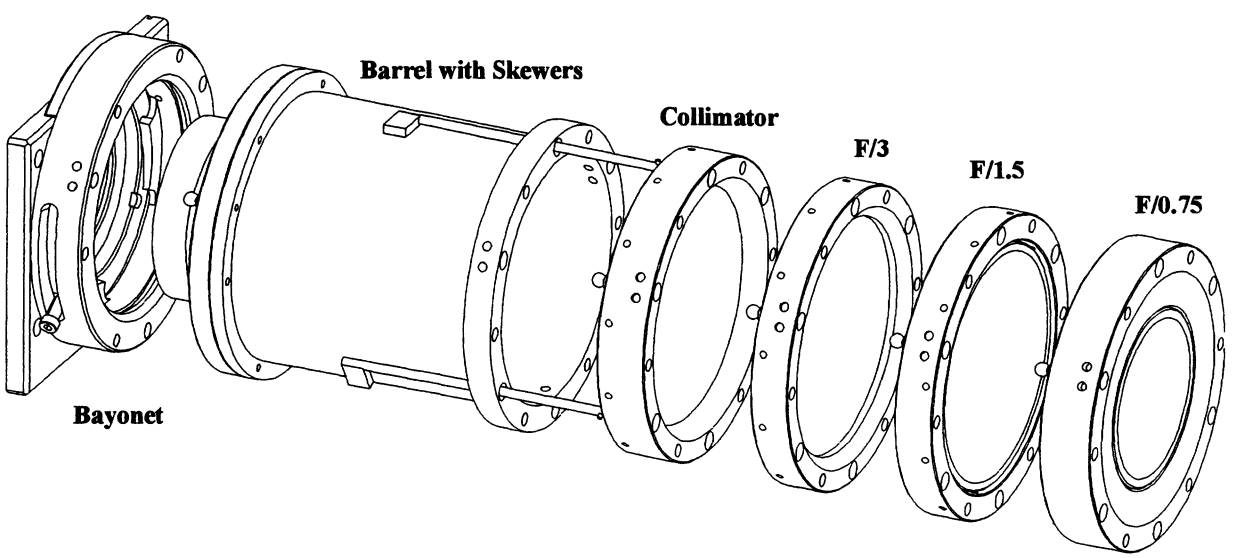

Figure 8. Accessory optics, exploded view.

path ghosts) is easily provided by the CGH. When stacked in other combinations, these elements produce a variety of aspheric test beams, hopefully easing the workload on the CGH null.

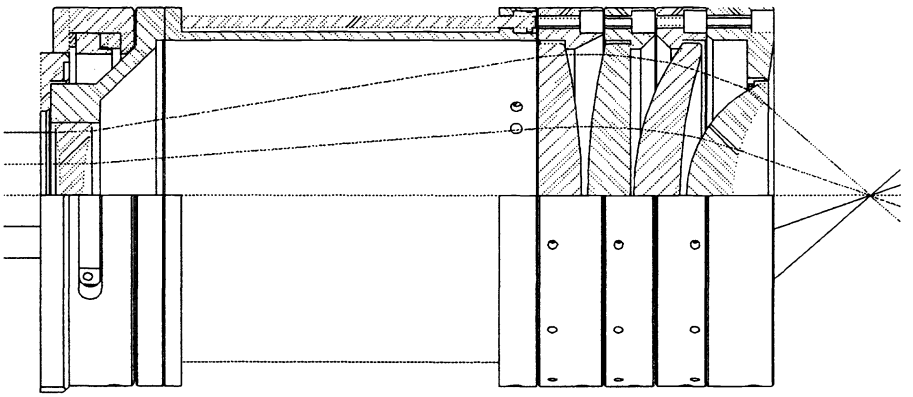

Figure 9. Accessory optics, sectional view.

The kinematic mounts consist of three shouldered tooling balls seated against three pairs of carbide rods. Stacking the accessory optics is best accomplished with the interferometer in an upward looking orientation, but each accessory includes 6 magnets of sufficient strength to hold it to an adjacent component and the barrel includes spring loaded skewers which can hold a stack of accessory optics onto the barrel in any orientation. The magnets hold the next accessory while the skewers are extended, so many hands are not required.

Each accessory optic can be thought of as comprise of three components: 1) a male kinematic mount, 2) a singlet lens and 3) a female kinematic mount. The relative alignment of these three components is easy to verify using only a dial gauge and spherical interferometer.

First, the alignment of the female kinematic mount relative to the male kinematic mount is determined by placing the accessory optic on a second stationary accessory optic with the tooling balls uppermost and clocking it through three (nominally) 120 degree increments. By measuring with a dial gauge the height of each tooling ball in one of the three locations relative to the stationary tooling ball beneath, we determine the relative tilt and axial displacement of the male versus female bayonets. By measuring the tangential location of each tooling ball in one of the three locations, we determine the relative decentration of the male versus female kinematic mounts. By measuring the tool ball tangential location relative to the ball beneath, we determine relative clock angle of the male versus female bayonets (although clock angle is probably not needed).

Next, we clock the accessory optic by 120 degree increments while observing an interferogram of one lens surface. The tilt, tip and focus fringes will determine the alignment of the optic surface relative to whichever bayonet was used, male or female. Repeat for the other optical surface. We can then construct a 4-surface raytrace model, beginning and ending with a dummy surface, which accounts for the mounting errors regardless of how the accessory optic is stacked with other components.

When the verifiable raytrace models of each accessory optic are combined with the verifiable raytrace model of the mainframe, we have everything we need to design a CGH aspheric null. The raytrace model begins with the test optic and ends with the CGH, which diffracts the wavefront to make it perfectly collimated. We can use the custom CGH to correct the known misalignments and aberrations of the various components. Alternatively, we can design the custom CGH assuming a perfect interferometer and accessory optics and then design a companion software null to correct the predicted aberrations. The later approach is preferred unless the predicted aberrations and misalignments are large enough to cause the interferogram to depart significantly from null.

4. DATA ACQUISITION AND ANALYSIS

A decision was made early on to develop entirely 32-bit software for Windows NT on a Pentium/PCI-bus system with the computer providing all the processing power. In retrospect this was the correct decision, but provided many pitfalls in the early stages of development. Initially we had difficulty finding a PCI-bus, RS-422 digital frame grabber with Windows NT drivers, and as a result the software evolved to have no specific hardware dependencies. Instead, all frame-grabber-specific functions are contained in dynamic link libraries, and we are able to support many different hardware configurations simply by providing additional libraries.

4.1 Phase Measuring Software—No Voodoo

Testing of deep aspherics often requires analyzing interferograms at higher camera resolutions than are supported by existing commercial software packages, and we want to know exactly what happens with the data. Consequently, we decided to develop our own phase measuring software, which we have named Durango. This software is thought to be unique in that it allows the user to optionally display and/or save the raw frame data, intensity, modulation and phase step maps instead of just the final phase map. We have also elected to use only published phase measuring algorithms and explicitly defined smoothing or data rejection algorithms to further reduce the "voodoo" element of computer-driven testing.

Figure 10 is a typical Durango screen dump. The interface is organized around a main data window that uses index tabs to access the various data maps including camera-frames, phase, intensity, modulation, phase step, and (soon) phase slope. Multiple data windows can be open simultaneously, displaying any part of the active data-set. Each window can be independently sized to display data at full or partial resolution. Cross-hairs can be dragged to change the location of cutting planes for cross-sectional views, and modulation and phase-step thresholds can be changed by graphical manipulation of cut-off points on histograms. Other optional windows can display system variables, measurement/analysis options and/or notes, and analysis results.

While our phase measuring algorithms are published, the computational details are not. By making extensive use of integer arithmetic, look-up tables, hash tables, and multithreading we are able to compute high resolution unwrapped phase maps very quickly. Execution times for computing and displaying modulation, phase, unwrap, peak-to-valley, and RMS using a 5-frame Hariharan algorithm[5] are shown in Table I. Because all processing is performed by the host computer, we can expect to compute phase maps approximately twice as fast by next year, even with no effort on our part (thanks to Intel). The multithreaded nature

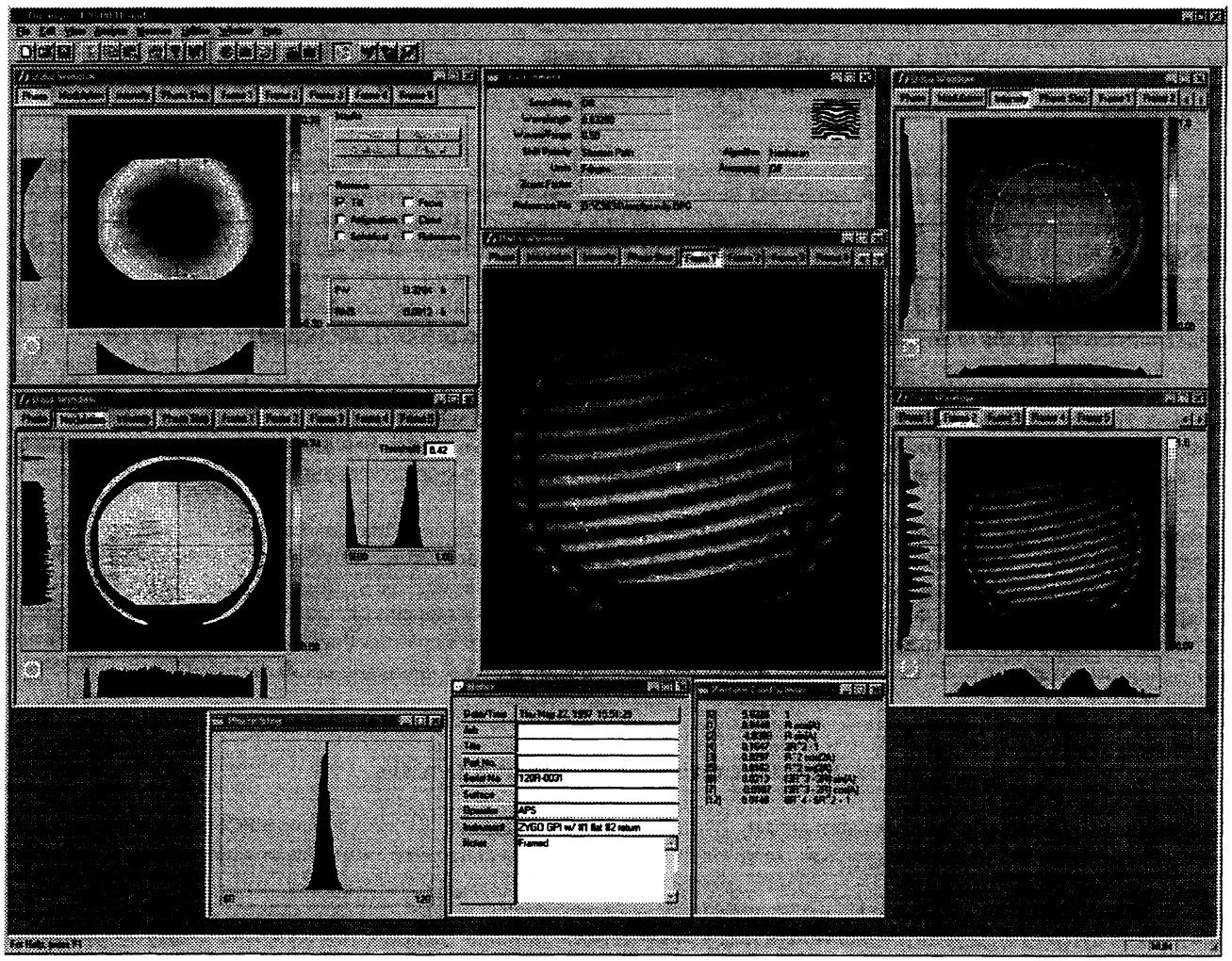

Figure 10. Durango phase measuring software.

of the application means that it is responsive to user input while the Pentium processor busily computes the results it anticipates the user will require. Computational threads are interrupted or restarted whenever user input renders them obsolete or irrelevant. The user never has to wait on the dreaded hourglass icon before redirecting a computation.

Table I. Circular aperture computation and display time using 5-frame Hariharan algorithm

Frame Size	Active Pixels	133 MHz Pentium	200 MHz Pentium Pro
1024 x 1024	823,500	10.6 sec	5.7 sec
512 x 512	205,800	2.6 sec	1.5 sec
256 x 256	51,400	0.67 sec	0.37 sec

In addition to its phase measuring capability, Durango permits hardware control through a multifunction IO board. Like the frame grabber boards, all code specific to the IO board is external to the application, enabling us to support multiple configurations with dynamic link libraries. Through this board we are able to control the interferometer zoom, focus, intensity, and reference mirror tilt.

5. CONCLUSION

We have designed and built a CGH-LUPI interferometer for the measurement of deep aspherics. This instrument meets our design objectives of measuring deep general aspherics, using prealigned photomask grade CGHs, and permitting verification of calibration without disassembly. The accuracy to which deep aspheres can be measured has yet to be demonstrated.

We have developed fast, high resolution phase measuring software for this instrument. Our goal of intelligent software which knows what is being measured and can correct for system aberrations in real time has not been achieved, but we are convinced our approach will take us there. A walkup aspheric test capability will require considerably more work.

ACKNOWLEDGMENT

This work was sponsored by NASA Goddard Space Flight Center under Contract NAS5-32808.

REFERENCES

1 J. E. Greivenkamp and J. H. Bruning, "Phase Shifting Interferometry", chapter 14 of *Optical Shop Testing*, ed. Daniel Malacara, John Wiley & Sons, 1992.

2 A.J. MacGovern and J.C. Wyant, "Computer generated holograms for testing optical element", Applied Optics **10**(3), 619-624, 1971.

3 Bernd Dörband and Hans J. Tiziani, "Testing aspheric surfaces with computer-generated holograms: analysis of adjustment and shape errors", Applied Optics 24(16), 2604-2611, 1985.

4 Steven M. Arnold, L. Curt Maxey, J. E. Rogers and R. C. Yoder, "Figure Metrology of Deep General Aspherics Using a Conventional Interferometer with CGH Null", SPIE Vol. **2536**, 106-116, 1995.

5 Greivenkamp and Bruning, *op. cit.*